Sensors & Actuators: B. Chemical 445 (2025) 138620

Contents lists available at ScienceDirect

Sensors and Actuators: B. Chemical

journal homepage: www.elsevier.com/locate/snb

Multifunctionalized PEG derivatives-based inverse opal photonic microspheres with a broad thermo operating window and pH responsiveness

Ran An [a,1], Penghui Li [a,1], Haizheng Li [a,b,1], Chunai Dai [a,*], Yuandu Hu [a,c,d,e,**]

[a] Department of Materials Science and Engineering, School of Physics Science and Engineering, Beijing Jiaotong University, Beijing 100044, China
[b] CRRC Changchun Railway Vehicles Co., Ltd, Changchun 130062, China
[c] Guangdong Provincial Key Laboratory of Technique and Equipment for Macromolecular Advanced Manufacturing, South China University of Technology, Guangzhou 510641, China
[d] Department of Chemical Engineering Tsinghua University, Beijing 100084, China
[e] Hubei Key Laboatory of Plasma Chemistry and Advanced Materials, Wuhan Institute of Technology, Wuhan 430205, China

ARTICLE INFO

Keywords:
PEG analogues
Hydrogel
Inverse opal
Thermo and pH-responsiveness
Broad thermal operating window

ABSTRACT

In the last decade, photonic structures based on responsive poly(ethylene glycol) (PEG)-analogues have drawn considerable attention. Nevertheless, the majority of reports concentrate on building 2D-like film-based photonic structures and lack multifunctionality. In this work, we report the construction of multifunctionalized PEG-analogues hydrogel-based photonic microspheres with an inverse opal structure. Opal-structured photonic microspheres (OSPMs) were firstly created using microfluidics-produced droplets of an aqueous dispersion of SiO_2 colloidal particles (CPs) as templates. The OSPMs were sequentially subjected to monomer infiltration, UV-induced polymerization and crosslinking, and wet etching of the SiO_2 CP building blocks, ultimately producing inverse opal photonic microspheres (IOPMs) with pH- and thermoresponsiveness. The IOPMs have a broad thermal operating window and can detect temperatures as high as 75 °C. The carboxylic acid groups in the skeleton of the IOPMs were further utilized to bind with positively charged compounds, such as ruthenium-functionalized polymers with fluorescence. The photonic microspheres are expected to show promising prospects in advanced sensing, visual temperature detection, anti-counterfeiting, and other related fields.

1. Introduction

Sensor is a device that can detect the information of objects and convert the information into electrical signals or other forms of outputs according to analytical rules [1,2]. Temperature, as an important physiological signal, can be used to evaluate the health status of our human body. Not only that, thermosensors also play an indispensable role in meteorological observation, agricultural planting, food safety, and other fields [3]. Hydrogels have excellent flexibility, biocompatibility and structural designability, and play an important role in the field of temperature sensing [4]. For example, Pang et al. developed a double network hydrogel composed of polyvinylpyrrolidone (PVP)/tannic acid (TA)/Fe^{3+} and a thermoresponsive poly (*N*-isopropylacrylamide-co-acrylamide) (P(NIPAAm-co-AM)) network. Temperature changes altered ion mobility, modulating the hydrogel's resistance [5]. Thermoresponsive hydrogels primarily monitor temperature changes by responding to mechanical variations and converting them into resistance changes, capacitance changes, or charge generation. However, there are issues with these conventional thermosensors, such as low detection efficiencies and the need for specialized and complex analytical equipments [6]. Inspired by the structural color changes of response photonic structures in our natural world, hydrogel-based photonic sensors have attracted extensive attention [7–11]. Though different building blocks, such as colloids, and linear

* Corresponding author.
** Corresponding author at: Department of Materials Science and Engineering, School of Physics Science and Engineering, Beijing Jiaotong University, Beijing 100044, China.
E-mail addresses: chadai@bjtu.edu.cn (C. Dai), huyd@bjtu.edu.cn (Y. Hu).
[1] These authors contributed equally.

https://doi.org/10.1016/j.snb.2025.138620
Received 26 March 2025; Received in revised form 27 August 2025; Accepted 27 August 2025
Available online 1 September 2025

polymers, can be employed to create various photonic structures, colloidal photonic structures have received the most attention because of their simple synthesis, easy for upscale production, and customized properties for a wide range of applications [12–16]. Research on photonic structures with multiple functions has increased due to the urgency of developing high-tech devices for multipurposes [17]. Polymer hydrogel-based inverse opal photonic structures have been the most extensively studied, despite photonic structures based on different colloidal building blocks and polymer matrix materials have been created [18,19]. This is because the copolymerization of monomers with different functionalities can easily yield diverse functionalized hydrogel-based photonic structures with distinct stimulus-responsive characteristics. Among them, one of the most studied photonic materials is hydrogel-based photonic structures with thermoresponsive properties [20–22]. NIPAAm has been frequently employed to create thermoresponsive photonic structures. However, the lower critical solution temperature (LCST) of PNIPAAm-based polymers at ~ 32 °C may limit their temperature operating window to a very narrow range, restricting their uses that require a wider temperature operating window [23–25]. Although other hydrophilic monomers can be copolymerized with NIPAAm and extend the resultant photonic structures' thermoresponsive temperature up to ~ 50 °C, the constraints in the thermal response range still exist [26–28]. Alternatively, researchers have found that another analogues of poly(ethylene glycol) (PEG) derivative-based thermoresponsive polymer hydrogels have a remarkable wider LCST range between 26 °C and 90 °C by changing the combination of the monomers [18,20,29,30]. Even though a few researchers have built PEG-based thermoresponsive photonic structures, they have mostly focused on bulk photonic structures or two-dimensional (2D) films [18,31], which generally exhibit angle-dependent structural colors that are undesired in many scenarios [32–34]. Comparably, spherical photonic structures have angle-independent properties because of their spherical symmetry, which expands their range of possible uses [35]. To date, multifunctional PEG-analogue hydrogel-based 3D photonic microspheres have yet to be realized. Therefore, it is anticipated to develop hydrogel-based thermoresponsive photonic microparticles with a broad thermoresponsive window and possess the capacity to integrate multiple functions [36].

In this work, we report the creation of multifunctional PEG-analogue hydrogel-based photonic microspheres with an inverse opal structure by combining the droplet microfluidics and templating method. To fabricate the microspheres, uniform droplets of an aqueous suspension of monodispersed SiO_2 CPs were fabricated by a glass capillary-based microfluidic device and collected and evaporated in a silicone oil. After solvent evaporation, the obtained opal-structured microspheres were submerged in a pregel solution containing PEG analogues (Oligo (ethylene glycol) methacrylate, $OEGMA_{360}$,), acrylic acid (AAc), and crosslinkers, followed by UV light irradiation, stripping, and wet etching of the SiO_2 CPs. The resultant inverse opal photonic microspheres (IOPMs) showed reversible responsive behaviors to temperature and pH stimuli. In particular, the microspheres have a wide temperature-responsive window between 20 and 75 °C, which is a significant boost when compared with conventional thermoresponsive photonic microspheres, and can be used as temperature sensors, especially in relatively high-temperature environments. Moreover, the negatively charged hydrogel skeleton P(OEGMA-co-AAc) can combine with a positively charged ruthenium polymer (pNIPAAm-*co*-$Ru(bpy)_3$) to give the microspheres new functions, such as fluorescence. As a proof-of-concept demonstration, these multifunctional IOPMs were further used as building blocks for various complex macrostructures, and showed great potential in the fields of advanced optical sensors and anticounterfeiting materials.

2. Experimental section

2.1. Materials

Ethanol (≥ 99.7 %), aqueous ammonia (≥ 28 %), tetraethyl orthosilicate (TEOS, electronic grade), hydrofluoric acid (HF), *N*-isopropylacrylamide (NIPAAm, 97 %), 2,2'-azobis(2-methyl propionitrile) (AIBN, 98 %), triethoxy-1H, 1 H, 2 H, 2H-tridecafluoro-n-octylsilane (TPFS, ≥ 99 %), acrylic acid (AAc), Oligo(ethylene glycol) methacrylate (OEGMA, M_n ~ 360), Di(ethylene glycol)methyl ether methacrylate (MEO_2MA), Ethylene glycol dimethacrylate (EGDMA), and pH buffer solutions (pH values of 2.00 ± 0.02, 4.60 ± 0.02, 7.00 ± 0.02, 9.6 ± 0.02, 12 ± 0.05) were purchased from Aladdin Co., Ltd (Shanghai, China). 2,2-diethoxy acetophenone (DEAP, > 95 %) was ordered from Sigma-Aldrich Co., Ltd (Shanghai, China). n-hexane was purchased from Shanghai Macklin Biochemical Co., Ltd (China). 4-Vinyl-4'-methyl-2,2'-bipyridine (99 %) was purchased from Ark Pharm, Inc (Libertyville, USA). Methyl-terminated fluorosilicone oil ($\rho = 1.266$ g/cm^3, 1000 cSt) was purchased from Xinan Chemical Co., Ltd (Zhejiang, China). Silicone oil (100 cSt) was purchased from Dow Corning (Shanghai, China). Ruthenium (4-vinyl-4'-methyl-2,2'-bipyridine)bis(2,2'-bipyridine) bis (hexafluoro phosphate) [denoted as $Ru(bpy)_3$] was synthesized accordingly [37]. Dialysis membrane tubing (MWCO: 8k−14k Da) was provided by Fisher Scientific, Inc (Shanghai, China). All the reagents were used as received.

2.2. Construction of microfluidic device

The microfluidic device consists of two circular glass capillaries (580 μm inner diameter (I.D.) and 1 mm outer diameter (O.D.), from World Precision Instruments, inc. (Shanghai)) and one square glass capillary with an inner dimension of 1.05 mm (wall thickness of 0.45 mm, from World Precision Instruments, inc. (Shanghai)). Briefly, a circular glass capillary tube was heated to form two blunt glass capillaries, and the blunt fracture was polished to obtain two circular capillaries with orifices of ~ 100 μm and ~ 350 μm, respectively. Then insert two circular capillaries into a square glass capillary tube, and the capillary with a larger orifice was used as an outlet collection tube. To ensure the stable generation of monodisperse emulsion droplets, the collection tube was treated by using the TPFS which can render the inner wall of the collection tube hydrophobic. Finally, we assembled them together using syringe needles and sealed them with epoxy resin adhesive to obtain microfluidic devices.

2.3. Synthesis and purification of SiO_2 CPs

The SiO_2 CP of various sizes was synthesized by the Stöber method [38]. Initially, 8 mL of aqueous ammonia ($NH_3{\cdot}H_2O$), 3 mL of deionized water, and a certain amount of ethanol were added to a conical flask. Then, 6 mL of TEOS was added and stirred at 60 °C at 500 rpm for the sol−gel process for 2 h. The particle size can be adjusted by changing the amount of ethanol. The product was centrifuged at 6000 rpm for 10 min and washed with water. The purified SiO_2 CP was dispersed in water for further use.

2.4. Fabrication of SiO_2 CP-based opal-structured microspheres and hydrogel-based inverse opal photonic microspheres

The SiO_2 CPs-based opal-structured microspheres were prepared by combining microfluidics with the solvent evaporation process. An aqueous suspension of SiO_2 CP (15 wt%) and silicone oil/methyl-terminated fluorosilicone oil (MFO) (5.5:1 v/v) was used as the dispersed and continuous phases. The flow rates of the inner aqueous phase and external oil phase were 100 and 3000 μL/h, respectively. The resultant emulsion droplets were collected into a hydrophobic polytetrafluoroethylene (PTFE) petri dish containing silicone oil (100 cSt)

(Fig. S1) and placed into an oven at 70 °C. After complete evaporation of water, the formed SiO_2 CP-based opal-structured photonic microspheres (OSPMs) were then washed with *n*-hexane to remove the silicone oil and calcined at 750 °C for 3 h to enhance their mechanical strength. Then, the calcined SiO_2 CP-based OSPMs were immersed in aqua regia for 6 h to remove any impurities and washed with deionized water, which was used as the template for fabrication of hydrogel-based inverse opal photonic microspheres (IOPMs). For the preparation of the IOPM, a series of steps were involved in the operation. First, 4.0 g of OEGMA, 0.2 g of AAc, 0.067 g of EGDMA, and 0.032 g of DEAP photoinitiator were dissolved in 16 mL of deionized water to prepare the pregel solution. Second, the OSPMs were immersed into the pregel solution for 24 h. After complete infiltration, they were placed between two glass slides with a certain thickness of spacer and irradiated with UV light (Gabon ZF-5, 16 W, Shanghai, China) for 30 min. After complete photopolymerization, the hydrogel film containing the microspheres was transferred to water, and the microspheres were separated by mechanical stripping; thus, individual composite photonic microspheres were obtained. The hydrogel-based photonic microspheres with inverse opal structure were obtained by immersing the composite microspheres in 10 % HF solution to remove the template of SiO_2 CP. After the etching process, the resultant microspheres were washed with deionized water three times. Therefore, IOPMs were obtained and stored in deionized water before use.

2.5. Synthesis of ruthenium-functionalized polymers (pNIPAAm-co-Ru(bpy)$_3$)

PNIPAAm-*co*-Ru(bpy)$_3$ copolymers were synthesized via free radical polymerization, as illustrated in Fig. S2. A 50 mL acetone/ethanol solution (1:9 v/v) of NIPAAm (5.1 g) and ruthenium monomer (0.52 g) was dissolved in a 100 mL Schlenk flask with a magnetic stir bar. Subsequently, 10 mL of ethanol solution containing 0.034 g of AIBN was added. After the solution was bubbled with N_2 for 30 min to remove dissolved oxygen, the polymerization was performed at 70 °C under N_2 for 6 h. The solution was bubbled with N_2 for 30 min to remove dissolved oxygen, followed by polymerization at 70 °C under an N_2 atmosphere for 6 h. The product was dialyzed against distilled water. ^{1}H NMR spectra and GPC traces of pNIPAAm-co-Ru(bpy)$_3$ were shown in Fig. S3.

2.6. Characterizations

Transmission electron microscopy (TEM) and scanning electron microscopy (SEM) images of SiO_2 CP were recorded on a TEM (JEOL, JEM-1400, Japan) and SEM (Hitachi S-4800), respectively. Morphologies of the SiO_2 CPs-based opal-structured microspheres were characterized by a scanning electron microscope (SEM, Hitachi S-4800 and SU8600, Japan). An optical microscope (Olympus Corporation, Olympus BX53M, China) was used to record the photonic microspheres under different modes of reflection, transmission, and fluorescence. Reflection spectra of the photonic microspheres were recorded under an Olympus microscope (reflection mode) equipped with a fiber optic spectrometer (USB Flame-S, Ocean Insight, Inc., China). The pH response was performed by immersing the inverse opal hydrogel photonic microspheres into the buffer solutions with different pH values. For the thermo-response test, an aqueous solution containing inverse opal hydrogel microspheres was heated with a customized hot table, and the reflection spectra and optical microscope images of the microspheres were recorded after stabilization. The zeta potential of pH buffer solution was measured by a Malvern Zetasizer Nano ZS90. ^{1}H NMR spectra were recorded by the Bruker Avance III HD spectrometer. For the sample preparation, d^6-DMSO was used as the solvent. Molecular weights of polymers were determined by gel permeation chromatography (GPC, Wyatt GPC/SEC-MALS system, Wyatt Technology Corporation, Santa Barbara, CA, USA) with 0.05 M LiBr DMF (HPLC grade) as the eluent.

3. Results and discussion

3.1. Preparation of PEG-analogue hydrogel-based IOPMs

Hydrogel-based IOPMs are prepared by combining the droplet microfluidics and templating techniques, as shown in Scheme 1. First, monodisperse SiO_2 CP-based opal-structured photonic microspheres (OSPMs) were obtained through the microfluidic technique and a subsequent solvent-evaporation process. An aqueous suspension of SiO_2 CP and silicone oil/MFO were used as the dispersed and continuous phases in a microfluidic device. The silicone oil phase sheared the aqueous suspension of SiO_2 CP into monodisperse emulsion droplets at an appropriate flow rate. At a given flow velocity of the dispersed phase at 300 μL/h but varied velocity of the continuous phase, the sizes of the droplets were greatly tunable (Fig. S4). The resulting emulsion droplets were then meticulously gathered in a PTFE petri dish that is hydrophobic, allowing the droplets to maintain their flawless spherical shape. The SiO_2 CP assembled to form a close-packed ordered structure with evaporation of the aqueous solution, yielding OSPMs. Then the calcination was introduced to improve the microspheres' mechanical strength (Fig. S5). P(OEGMA-co-AAc) hydrogel-based IOPMs were prepared by filling the voids within the OSPMs with a pregel solution, UV-irradiated for in-situ polymerization, and followed by HF etching of the SiO_2 CP templates. Since the hydrogel skeleton was negatively charged, the hydrogel-based IOPMs were further functionalized with positively charged linear polymers, such as pNIPAAm-*co*-Ru(bpy)$_3$, through the electrostatic interaction.

The diameter of SiO_2 CP determines the structural hue of OSPMs. The OSPMs with different structural colors from blue (Fig. S6a) to light-blue (Fig. 1a) to green (Fig. S6b) were obtained by using SiO_2 CP of 210 nm, 256 nm, and 288 nm (Fig. S7). We took the light-blue OSPM for an example. On the exterior and inside of the OSPM, the SiO_2 CPs are neatly arranged in a hexagonal array (Fig. 1b, c and Fig. S8). SiO_2 CP-hydrogel composite photonic microsphere (CPM) with green color was produced (Fig. 1d) following the introduction of the hydrogel skeleton that was through the polymerization of the monomers $OEGMA_{360}$ and AAc. The CPM exhibited a reflection peak at 512 nm (Fig. 1g). Subsequently, the CPM was placed in an HF solution to remove the template. The initial green CPM was transformed into a yellow IOPM in this process (Fig. 1e, f). The optical microscopy images of the OSPM at different stages of the etching process were shown in Fig. S9. It can be clearly seen that the size of the CPM gradually increased from 362 μm to 447 μm as etching progressed. In the CPM, the polymer skeleton was constrained by tightly packed SiO_2 CPs. After the etching process, the constraint was dismissed, which also caused a change in refractive index. Additionally, the hydrogel skeleton can absorb a large amount of water, leading to the size expansion and an increase in lattice spacing. The synergistic effect caused a red-shift in the photonic microsphere, and the reflection peak shifted from 512 nm to 580 nm (Fig. 1g). The molecular structure of P(OEGMA-co-AAc) was shown in Fig. 1h. The hydrogel-based IOPMs have a uniform particle size, indicating that the microfluidic technique has good stability (Fig. S10). The bright structural colors of IOPMs can be visualized (Fig. S11) and have the potential to be used as photonic pigments. Fig. 1i illustrates the transformation of the SiO_2 CP-hydrogel CPM into a hydrogel-based IOPM. Fig. S12 shows the preparation process of the hydrogel-based IOPM using a blue-colored OSPM as the template, demonstrating similar changes.

3.2. Temperature and pH response of PEG-analogues hydrogel-based IOPMs

Since Asher et al. reported the polymerized colloidal crystal array as a pH sensor, photonic crystals have shown a promising potential for the stimuli-responsive chemical sensors [39]. Responsive photonic crystals with tunable photonic bandgaps that were generated from an ordered microstructure enable dynamic structural color variation in response to

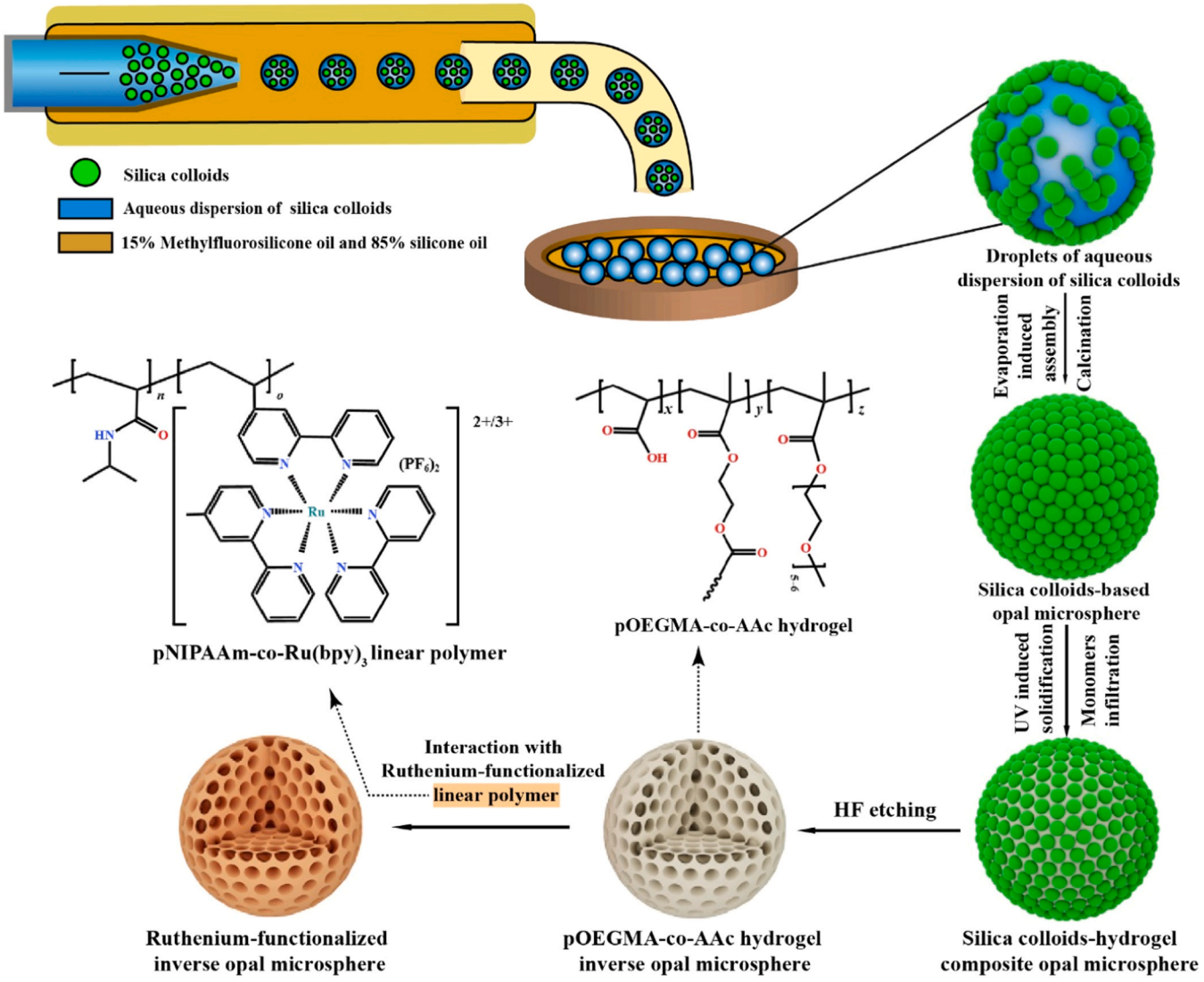

Scheme 1. Schematic of the construction of PEG-analogue hydrogel-based IOPMs and the ruthenium compound functionalization process.

external stimuli. Thermochromic materials, which can dynamically and reversibly change color with temperature, have great potential in applications such as sensors, displays, and anti-counterfeiting [40]. The copolymers of PEG derivatives are ideal candidates because of their excellent biocompatibility, tunable LCST, and antifouling properties when compared with PNIPAM hydrogel [41]. P(OEGMA-co-AAc) hydrogel-based photonic microspheres with an inverse opal structure were initially created by combining microfluidic and templating methods. Because of the presence of functional groups like OEGMA (thermosensitive group) and AAc (pH-sensitive group), the photonic microspheres exhibit dual responsiveness to temperature and pH. Fig. 2a shows optical microscopy images of an IOPM in water at varying temperatures, and the corresponding reflection spectra are shown in Fig. 2b. The photonic microsphere's structural hue shifted from green to yellow as the temperature increased from 20 °C to 75 °C. Meanwhile, the photonic microsphere underwent deswelling, with its size shrinking from ~ 620 μm to ~ 554 μm. The λ_{max} moved from 580 nm to 513 nm due to a blue shift in structural hue brought on by the reduction in lattice spacing. The IOPM's λ_{max} and relative swelling ratio (D/D_0) are displayed as a function of temperature in Fig. 2c, and both exhibit a comparable change tendency. Notably, when the temperature rose above 70 °C, the reflection spectra showed a significant blue shift, suggesting that the current temperature is near the LCST of P(OEGMA-co-AAc) hydrogel. The P(OEGMA-co-AAc) hydrogel is hydrophilic at temperatures below the LCST, which favors the formation of hydrogen bonds between the hydrophilic groups and water molecules. These hydrogen bonds gradually deteriorate as the temperature rose, and when the temperature surpassed the LCST, the hydrogen bonds between the polymer chain and water molecules were broken, causing P(OEGMA-co-AAc) hydrogel to undergo a conformational transition from a hydrophilic state to a hydrophobic state. As a result, the IOPM contracted rapidly, and the reflection spectra quickly shifted to blue at the temperature close to the LCST [42]. Neat PNIPAM hydrogel-based IOPMs typically lose their structural color around 32 °C [27], while P(OEGMA-co-AAc) microspheres have a broad thermochromic range up to 75 °C, increasing their potential applications, such as sensors for relatively higher temperature environments. The IOPMs' thermoresponse mechanism due to temperature change is illustrated in Fig. 2d. As shown in Fig. 2e, we filled the 'BJTU' (Beijing Jiaotong University) groove with green and red IOPMs (Fig. S13) as building blocks, producing a remarkable structural color pattern. Additionally, the hue of the pattern 'BJTU' can be adjusted by the variations of ambient temperature, for example the hue change from yellow-green to blue-green (as shown in Supplementary Material Video S1). IOPMs can be used as building blocks for various shapes, allowing macroscopic observation of temperature changes. The 'BJTU' pattern changed from its initial

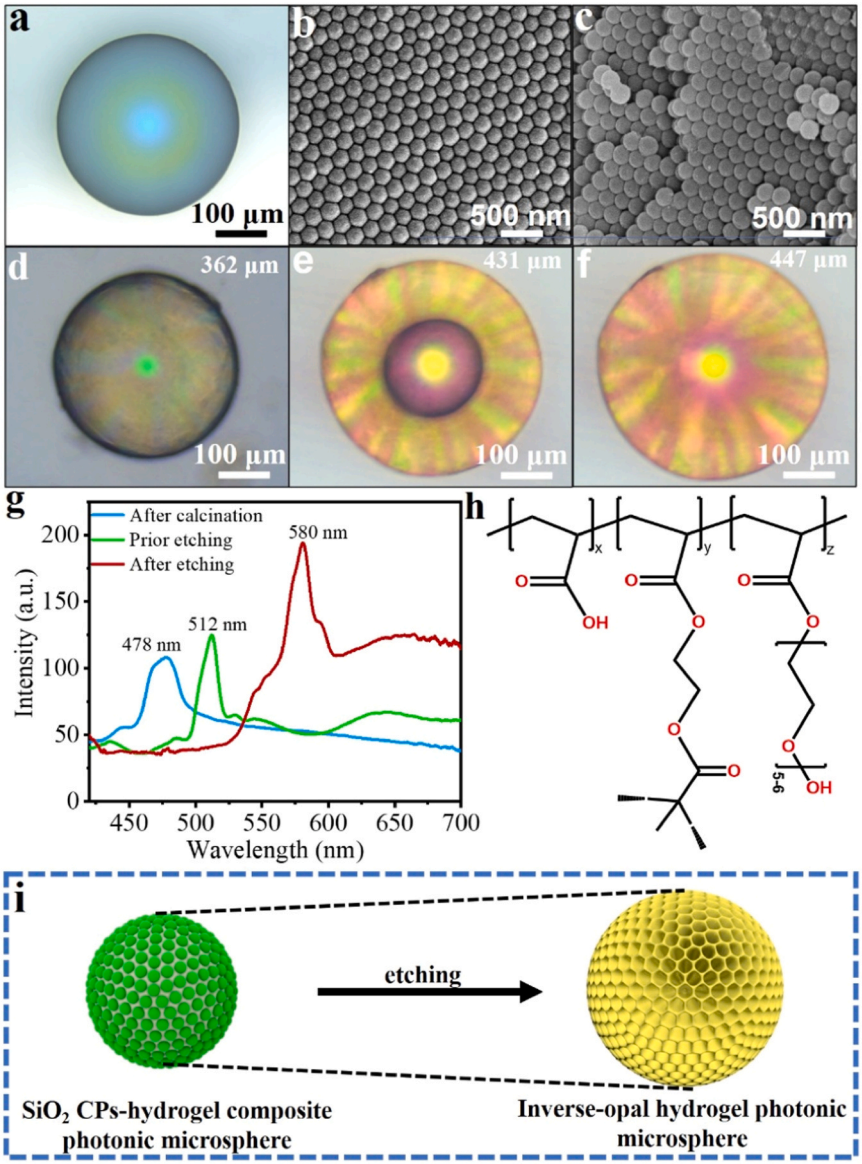

Fig. 1. (a) Optical microscopy image of a light-blue OSPM. SEM images of the surface (b) and cross-section (c) of the OSPM. Optical microscopy images of the CPM before (d), in the middle of (e), and after (f) etching. (g) Reflection spectra of the photonic microsphere at different stages. (h) Molecular structure of P(OEGMA-co-AAc). (i) Schematic structure of the CPM before and after etching.

red/green color to a green/blue color as the temperature rose and then returned to its original color when the temperature dropped back to room temperature. This change is clear and intuitive, easily recognizable by the naked eye. Fig. 2f shows a schematic of the 'BJTU' groove filled with photonic microspheres at 25 °C and 75 °C.

In addition to the thermoresponse, the hydrogel-based IOPMs can also react to different pH values because of the AAc groups. As shown in Fig. 3a and Fig. S14, the hydrogel-based IOPM turned red when the pH value rose from 2 to 12, and the stopband position showed a red-shift of about 40 nm (Fig. 3b). The microsphere expanded as the pH increased, and this pattern was in line with the λ_{max} variation (Fig. 3c). The structural color and reflection spectra of the photonic microsphere didn't significantly change when it was built using OEGMA as the sole monomer (Fig. S15). Thus, it can be concluded that the polar carboxyl groups are responsible for the photonic micrispheres' pH reactivity. The pH range of 4.6–7 was where the hydrogel-based IOPM showed the highest reactivity. At 25 °C, however, because of electrostatic interactions between monomer units, the real pKa of AAc within the hydrogel was likely to be somewhat higher [43]. The protonated PAAc was uncharged in the solution with a pH of 2, but as the pH rose beyond 4.6 (higher than pKa), carboxyl groups deprotonated to produce negative charges (Fig. S16). The strong charge repulsion in the hydrogel raised the gel's internal osmotic pressure, which caused the hydrogel-based IOPM to expand and the lattice spacing to widen. This caused the reflection spectra to redshift. However, because the change in the concentration of the combined charge in the hydrogel can be ignored, the photonic microsphere was nearly insensitive when the pH was higher than 7 [44]. In addition, the photonic microspheres also exhibit temperature responsiveness at different pH values (Fig. S17). Experimental results revealed that the photonic microspheres responded to changes in temperature and pH by varying their volume. The ordered pores endowed the photonic microspheres with a photonic stopband and corresponding characteristic reflection peaks. Under normal incidence, the peak positions λ of the microspheres can be estimated by Bragg's equation [45]:

$$\lambda = 1.633 d n_{average} \quad (1)$$

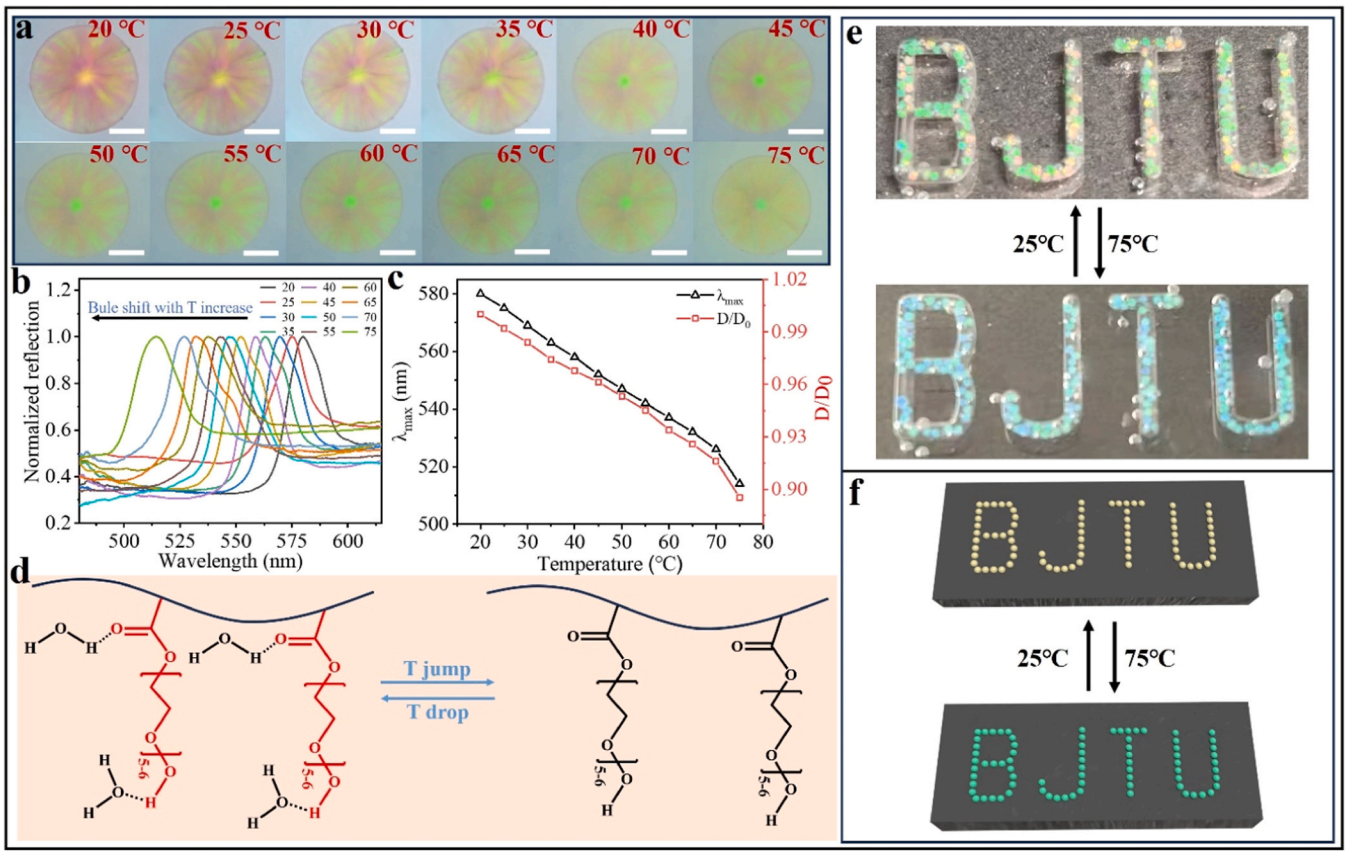

Fig. 2. Optical microscopy images (a) and corresponding reflection spectra (b) of the P(OEGMA—co-AAc) hydrogel-based IOPM at different temperatures. The scale bar is 200 μm. (c) λ_{max} and relative swelling ratio (D/D_0, where D_0 and D are the initial and varied diameters of the IOPM, respectively) of the IOPM as a function of temperature. (d) Schematic diagram of the response mechanism of the IOPM under different temperature conditions. (e-f) Photographs and schematic illustrations of the 'BJTU' pattern filled with photonic microspheres at 25 °C and 75 °C.

where d is the center-to-center distance between two neighboring nanopores, and $n_{average}$ is the average refractive index of the system. Obviously, with the change of swelling degree, the diameter of pores was changed accordingly. λ can shift in relation to the change in d. Therefore, when photonic microspheres are stimulated by different temperatures or pH, the structural color can change accordingly.

For the creation of high-performance photonic sensors, batch-to-batch consistency and reversibility are crucial. The photonic microspheres from different batches exhibited similar sensing performance, as shown in Fig. S18. The IOPM's temperature and pH stability were measured within 10 cycles, as shown in Fig. S19. Throughout the cycle process, the IOPM showed only minor variations in λ_{max}, demonstrating good reversibility and sufficient stability. In addition, we found that the size of photonic microspheres don't affect the sensing performance (Fig. S20 and S21).

3.3. Functionalization of PEG-analogue hydrogel-based IOPMs

The IOPMs were made with a negatively charged P(OEGMA-co-AAc) hydrogel skeleton. This feature can be used to incorporate different functional materials into the particular photonic microsphere. Ruthenium-functionalized linear polymers, such as pNIPAAm-*co*-Ru(bpy)$_3$ (Fig. 4a), have been extensively studied due to their multifunctional responsive characteristics, including thermoresponsiveness, catalysis, and fluorescence performance [46]. When the IOPMs were submerged in an aqueous solution containing ruthenium-functionalized polymers, the microspheres were functionalized because the polymers were firmly adsorbed onto them by electrostatic interactions. The metal-to-ligand charge transfer (MLCT) effect causes ruthenium-functionalized polymers to appear orange in aqueous solution [47], which in turn causes the modified photonic microspheres to be adorned in an orange hue (Fig. 4b, d). The photonic microsphere was initially yellow under reflection mode, but after functionalization it turned to red (Fig. 4c, e). The maximum reflection peak of the photonic microsphere shifted from 570 nm to 605 nm, further confirming the change in structural color (Fig. 4g). This was probably caused by the addition of the linear polymers, which can increase the osmotic pressure within the hydrogel skeleton. As a result, the diameter of the functionalized photonic microsphere was increased by 3.8 %, and the lattice spacing changed accordingly. The incorporation of ruthenium-functionalized polymers resulted in fluorescence properties (Fig. 4f) and great fluorescence stability, which can be maintained in water for over one month (Fig. S22). Interestingly, under fluorescence mode, it is impossible to discern between ruthenium-functionalized IOPMs with different structural hues. This original structural color information was successfully obscured by this (Fig. S23). Applications such as encrypting or anti-counterfeiting are anticipated for these photonic microspheres. We filled the functionalized IOPMs into a 'BJTU' groove with two distinct colored microspheres that are visible. The design displayed a consistent brilliant red fluorescence when exposed to UV light (Fig. 4h). The schematic diagram of the 'BJTU' groove filled with the ruthenium-functionalized IOPMs under UV light is shown in Fig. 4i.

4. Conclusion

In conclusion, droplet microfluidics and templating method were successfully combined to create multifunctional P(OEGMA-co-AAc)

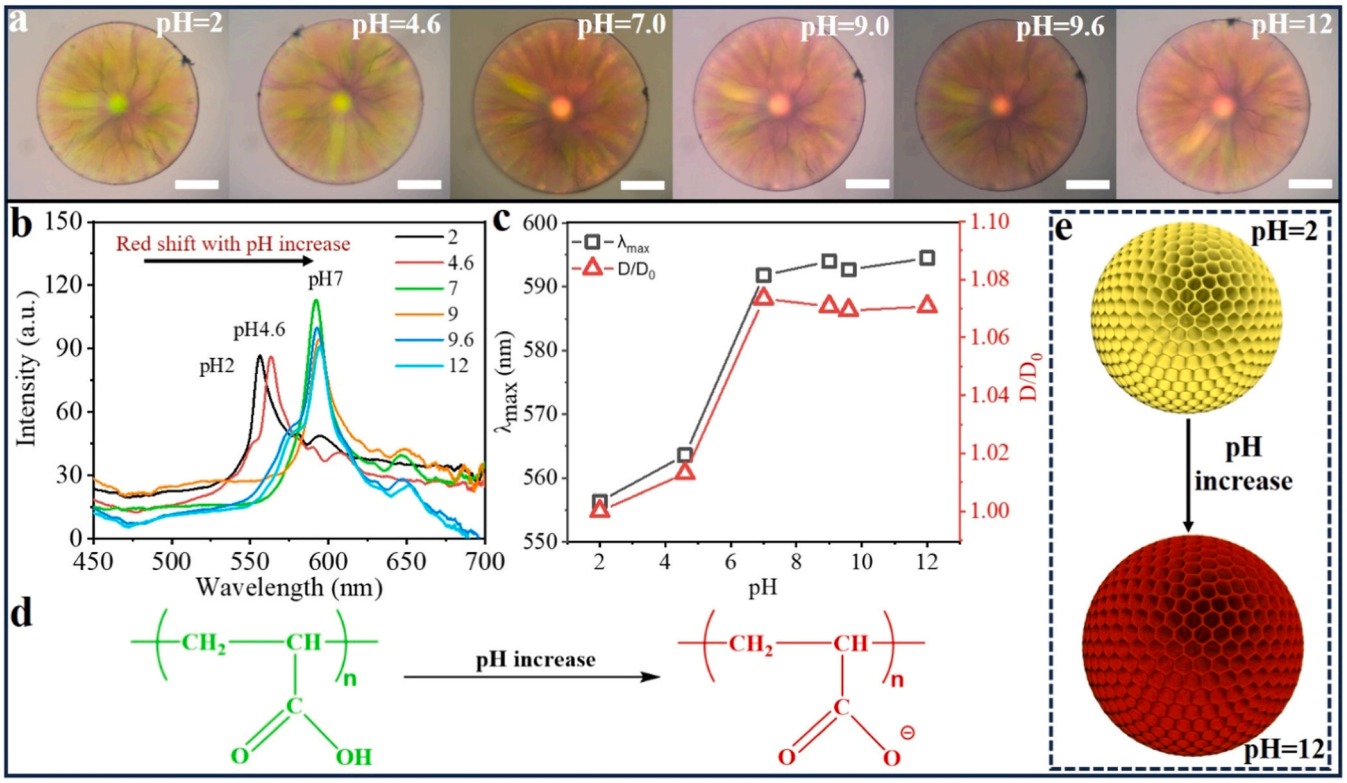

Fig. 3. The IOPM under various pH levels is shown in optical microscopy images (a) and matching reflection spectra (b). The scale bar is 200 μm. (c) The P(OEGMA-co-AAc) hydrogel-based IOPM's λ_{max} and relative swelling ratio in relation to pH. (d) Diagrammatic representation of the IOPM's response mechanism in both acidic and basic environments. (e) Diagrammatic representation of the IOPM in both acidic and basic conditions.

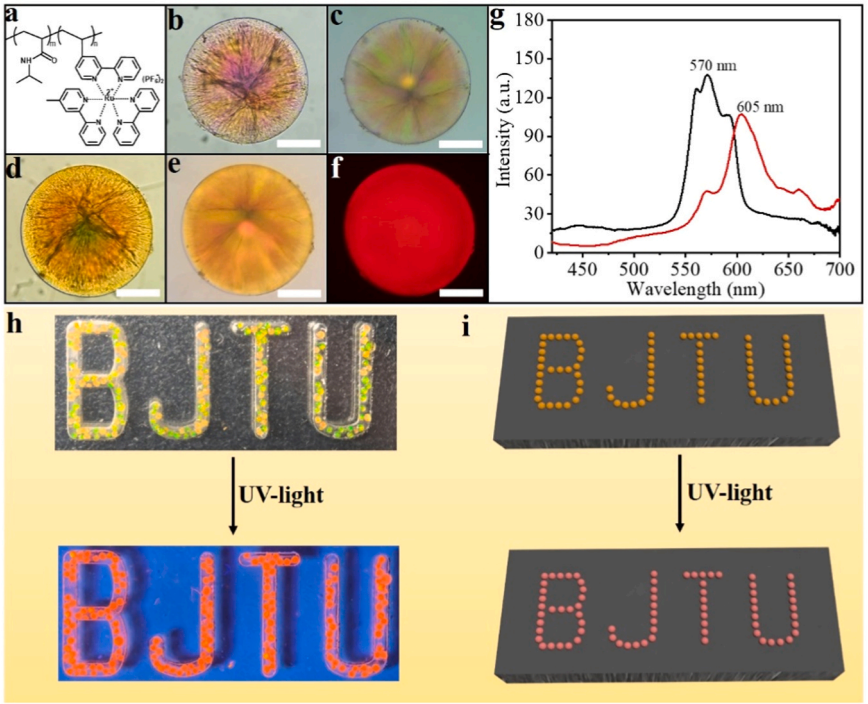

Fig. 4. (a) Chemical structure of the ruthenium-functionalized polymer. A P(OEGMA-co-AAc) hydrogel-based IOPM was photographed using optical microscopy both before (b, c transmission and reflection modes) and after (d, e transmission and reflection modes) a 24 h immersion in the ruthenium-functionalized polymer solution. (f) The IOPM imaged by fluorescence microscopy. The scale bar is 200 μm. (g) Reflection spectra of the IOPM before and after the ruthenium polymers' labeling. (h-i) Images and a schematic representation of the 'BJTU' groove filled with the ruthenium-functionalized IOPMs under white and UV light.

hydrogel-based photonic microspheres with an inverse opal structure. To achieve this, uniform OSPMs were firstly created using monodisperse SiO_2 CPs as the building blocks, and were subsequently submerged in a pregel solution containing OEGMA and AAc monomers. UV-induced polymerization created SiO_2 CPs-hydrogel composite microspheres, which were then treated with HF to remove SiO_2 CP templates, resulting in hydrogel-based IOPMs. These microspheres exhibit a dual response to temperature and pH, as well as exceptional stability and reversibility. In particular, they outperform conventional pNIPAAm hydrogel-based thermochromic microspheres, responding within a broad temperature range (20–75 °C) while retaining a vibrant structural color, effectively broadening their range of applications, such as serving as sensors for environments with relatively higher temperatures. The photonic microspheres can also be used as the building blocks of patterns for macroscopic temperature monitoring. Additionally, because of the negatively charged nature of the IOPMs' polymer skeleton, positively charged ruthenium-functionalized polymers, pNIPAAm-*co*-Ru(bpy)$_3$ were easily bonded to photonic microspheres through the electrostatic interaction, giving them fluorescence characteristics. These multifunctional hydrogel-based IOPMs, in our opinion, have applications in anti-counterfeiting, display, and sensing.

CRediT authorship contribution statement

Yuandu Hu: Writing – review & editing, Validation, Supervision, Funding acquisition, Conceptualization. **Ran An:** Validation, Methodology, Investigation, Data curation, Conceptualization. **Penghui Li:** Writing – original draft, Visualization, Methodology, Investigation, Data curation. **Haizheng Li:** Methodology, Investigation, Data curation. **Chunai Dai:** Validation, Formal analysis.

Declaration of Competing Interest

The authors declare that they have no known competing financial interests or personal relationships that could have appeared to influence the work reported in this paper.

Acknowledgements

This work is supported by Fundamental Research Funds for the Central Universities (No. 2025JBZX005 (Y. H.), No. 2024YJS195 (P. L.) No. 2025YJS186 (R. A.)). Y. H. is grateful for the funds from the Guangdong Provincial Key Laboratory of Technique and Equipment for Macromolecular Advanced Manufacturing (No. 20240518), the Key Laboratory of Advanced Materials of Ministry of Education (No. Advmat-2402), and the Hubei Key Laboatory of Plasma Chemistry and Advanced Materials (No. 2024P04).

Appendix A. Supporting information

Supplementary data associated with this article can be found in the online version at doi:10.1016/j.snb.2025.138620.

Data Availability

Data will be made available on request.

References

[1] T. Li, G. Liu, H. Kong, G. Yang, G. Wei, X. Zhou, Recent advances in photonic crystal-based sensors, Coord. Chem. Rev. 475 (2023) 214909.
[2] J. Wang, M. Yokokawa, T. Satake, H. Suzuki, A micro IrO_x potentiometric sensor for direct determination of organophosphate pesticides, Sens. Actuators B Chem. 220 (2015) 859–863.
[3] C. Tang, Y. Wang, Y. Li, S. Zeng, L. Kong, L. Li, J. Sun, M. Zhu, T. Deng, A review of graphene-based temperature sensors, Microelectron. Eng. 278 (2023) 112015.
[4] L. Shao, M. Liu, J. Qiu, C. Gao, G. Zhang, L. Qin, Preparation of conductive hydrogel, Prog. Chem. 23 (2011) 923–929.
[5] Q. Pang, H. Hu, H. Zhang, B. Qiao, L. Ma, Temperature-responsive ionic conductive hydrogel for strain and temperature sensors, ACS Appl. Mater. Interfaces 14 (2022) 26536–26547.
[6] F. Mo, P. Zhou, S. Lin, J. Zhong, Y. Wang, A review of conductive hydrogel-based wearable temperature sensors, Adv. Healthc. Mater. 13 (2024) 2401503.
[7] J. Geng, K. Shao, P. Zhang, C. Chen, S. Huang, Advances in photonic crystal hydrogels for biomedical research: a review, J. Biotechnol. 404 (2025) 162–174.
[8] X. Lu, B. Han, D. Wei, M. Chu, H. Ma, R. Li, X. Hou, Y. Zhang, J. Wang, A fluorescence-enhanced inverse opal sensing film for multi-sources detection of formaldehyde, Food Sci. Hum. Wellness 14 (2025) 9250115.
[9] M. Pan, M. Gao, J. Cui, R. Gao, H. Li, J. Sun, W. Chen, S. Wang, Fluorescent molecularly imprinted hydrogel sensing strip based on nitrogen-doped carbon dots and inverse opal photonic crystals applying for effective detection for imidacloprid in fruits and vegetables, Food Chem. 477 (2025) 143497.
[10] M. Pan, Y. Wang, J. Yang, H. Li, X. Han, S. Wang, Carbon dots-based fluorescent molecularly imprinted photonic crystal hydrogel strip: portable and efficient strategy for selective detection of tetracycline in foods of animal origin, Food Chem. 433 (2024) 137407.
[11] F. Zhao, X. Liu, X. Li, Z. Cai, Y. Zhang, Two-dimensional photonic crystal acetylcholinesterase hydrogel and organohydrogel sensors for efficient detection of organophosphorus compounds, Biosens. Bioelectron. 267 (2025) 116845.
[12] Q. Guo, R. Xue, J. Zhao, Y. Zhang, G.T. van de Kerkhof, K. Zhang, Y. Li, S. Vignolini, D. Song, Precise tailoring of polyester bottlebrush amphiphiles toward eco-friendly photonic pigments via interfacial self-assembly, Angew. Chem. Int. Ed. 61 (2022) e202206723.
[13] S.H. Han, Y.H. Choi, S.-H. Kim, Co-assembly of colloids and eumelanin nanoparticles in droplets for structural pigments with high saturation, Small 18 (2022) 2106048.
[14] Z. Cai, Z. Li, S. Ravaine, M. He, Y. Song, Y. Yin, H. Zheng, J. Teng, A. Zhang, From colloidal particles to photonic crystals: advances in self-assembly and their emerging applications, Chem. Soc. Rev. 50 (2021) 5898–5951.
[15] B. Wang, K. Zhang, P. Li, Y. Li, D. Song, Scalable and precise synthesis of structurally colored bottlebrush block copolymers: enabling refined color calibration for sustainable photonic pigments, Angew. Chem. Int. Ed. 64 (2025) e20242131.
[16] Y. Hu, A. Ardekani, J. Zhu, Y. Yang, J. Pérez-Mercader, Droplet microfluidics, colloidal assembly and nanoscale processing: synergistic control and properties of colloid-based photonic microobjects, Adv. Colloid Interface Sci. 344 (2025) 103601.
[17] Z. Yang, Albrow-Owen, W. Cai, T. Hasan, Miniaturization of optical spectrometers, Science 371 (2021) eabe0722.
[18] J.-P. Couturier, M. Suetterlin, A. Laschewsky, C. Hettrich, E. Wischerhoff, Inverse opal hydrogels for the sensing of macromolecules, Angew. Chem. Int. Ed. 54 (2015) 6641–6644.
[19] H. Wang, Y. Liu, Z. Chen, L. Sun, Y. Zhao, Anisotropic structural color particles from colloidal phase separation, Sci. Adv. 6 (2020) eaay1438.
[20] Y. Wu, R. Sun, Y. Han, S. Zhang, S. Wu, Ultrathin photonic crystal film with supersensitive thermochromism in air, Chem. Eng. J. 451 (2023) 139075.
[21] T. Kanai, N. Kobayashi, H. Tajima, Enhanced linear thermosensitivity of gel-immobilized colloidal photonic crystal film bound on glass substrate, Mater. Adv. 2 (2021) 2600–2603.
[22] Y. Hu, J. Wang, H. Wang, Q. Wang, J. Zhu, Y. Yang, Microfluidic fabrication and thermoreversible response of core/shell photonic crystalline microspheres based on deformable nanogels, Langmuir 28 (2012) 17186–17192.
[23] T. Kanai, D. Lee, H.C. Shum, R.K. Shah, D.A. Weitz, Gel-immobilized colloidal crystal shell with enhanced thermal sensitivity at photonic wavelengths, Adv. Mater. 22 (2010) 4998–5002.
[24] K. Matsubara, M. Watanabe, Y. Takeoka, Thermally adjustable multicolor photochromic hydrogel, Angew. Chem. Int. Ed. 46 (2007) 1688–1692.
[25] M. Chen, L. Zhou, Y. Guan, Y. Zhang, Polymerized microgel colloidal crystals: photonic hydrogels with tunable band gaps and fast response rates, Angew. Chem. Int. Ed. 52 (2013) 9961–9965.
[26] J. Wang, Y. Hu, R. Deng, R. Liang, W. Li, S. Liu, J. Zhu, Multiresponsive hydrogel photonic crystal microparticles with inverse-opal structure, Langmuir 29 (2013) 8825–8834.
[27] Z. Jia, R. Xie, Y. Hu, X. Ju, W. Wang, Z. Liu, L. Chu, Thermochromic photonic crystal microspheres with uniform color display and wide coloration range, Macromol. Rapid Commun. 44 (2023) 2200800.
[28] T. Wang, J. Liu, F. Nie, Non-dye cell viability monitoring by using pH-responsive inverse opal hydrogels, J. Mater. Chem. B 6 (2018) 1055–1065.
[29] T. Cai, G. Wang, S. Thompson, M. Marquez, Z. Hu, Photonic hydrogels with poly (ethylene glycol) derivative colloidal spheres as building blocks, Macromolecules 41 (2008) 9508–9512.
[30] J.-F. Lutz, Polymerization of oligo(ethylene glycol) (meth)acrylates: toward new gnerations of smart biocompatible materials, J. Polym. Sci. A Polym. Chem. 46 (2008) 3459–3470.
[31] Y. Wu, R. Sun, J. Ren, S. Zhang, S. Wu, Bioinspired dynamic camouflage in programmable thermochromic-patterned photonic films for sophisticated anti-counterfeiting, Adv. Funct. Mater. 33 (2023) 2210047.
[32] S. Yu, D. Ma, C. Qi, D. Yang, S. Huang, All-in-one photonic crystals with multi-stimuli-chromic, color-recordable, self-healable, and adhesive functions, Adv. Funct. Mater. 34 (2024) 2411670.
[33] C. Chi, D. Zhang, X. Xu, J. Li, J. Ren, X. Xu, J. Xian, H. Chen, H. Jameel, Angle-dependent and liquid-responsive photonic crystals for anti-counterfeiting and optical sensing, CrystEngComm 27 (2025) 1910–1917.

[34] Y. Zhao, L. Shang, Y. Cheng, Z. Gu, Spherical colloidal photonic crystals, Acc. Chem. Res. 47 (2014) 3632–3642.
[35] J. Wang, J. Zhu, Recent advances in spherical photonic crystals: generation and applications in optics, Eur. Polym. J. 49 (2013) 3420–3433.
[36] K. Zhou, T. Tian, C. Wang, H. Zhao, N. Gao, H. Yin, P. Wang, B.J. Ravoo, G. Li, Multifunctional integrated compartment systems for incompatible cascade reactions based on onion-like photonic spheres, J. Am. Chem. Soc. 142 (2020) 20605–20615.
[37] Z. Fang, S. Keinan, L. Alibabaei, H. Luo, A. Ito, T.J. Meyer, Controlled electropolymerization of ruthenium(II) vinylbipyridyl complexes in mesoporous nanoparticle films of TiO_2, Angew. Chem. Int. Ed. 53 (2014) 4872–4876.
[38] W. Stöber, A. Fink, E. Bohn, Controlled growth of monodisperse silica spheres in the micron size range, J. Colloid Interface Sci. 26 (1968) 62–69.
[39] K. Lee, S.A. Asher, Photonic crystal chemical sensors: ph and ionic strength, J. Am. Chem. Soc. 122 (2000) 9534–9537.
[40] C. Wei, X. Lu, X. Wen, Y. Liu, S. Yang, Thermo-responsive color-changeable photonic materials: a review, Opt. Laser Technol. 152 (2022) 108135.
[41] L. Hou, P. Wu, Microgels with linear thermosensitivity in a wide temperature range, Macromolecules 49 (2016) 6095–6100.
[42] W. Zhao, M. Quan, Z. Cao, Y. Zhang, J. Wen, D. Pan, Z. Dong, Z. Yang, D. Wang, H. Cao, W. He, Visual multi-triggered sensor based on inverse opal hydrogel, Colloids Surf. A 554 (2018) 93–99.
[43] M. Ben-Moshe, V.L. Alexeev, S.A. Asher, Fast responsive crystalline colloidal array photonic crystal glucose sensors, Anal. Chem. 78 (2006) 5149–5157.
[44] J. Shin, S.G. Han, W. Lee, Inverse opal ph sensors with various protic monomers copolymerized with polyhydroxyethylmethacrylate hydrogel, Anal. Chim. Acta 752 (2012) 87–93.
[45] B. Ye, H. Ding, Y. Cheng, H. Gu, Y. Zhao, Z. Xie, Z. Gu, Photonic crystal microcapsules for label-free multiplex detection, Adv. Mater. 26 (2014) 3270–3274.
[46] D. Suzuki, T. Sakai, R. Yoshida, Self-flocculating/self-dispersing oscillation of microgels, Angew. Chem. Int. Ed. 47 (2008) 917–920.
[47] J.-L. Fillaut, Ruthenium(II) polypyridyl complexes as two-photon absorbers and sensitizers: design, structure-properties relationships and applications, Coord. Chem. Rev. 518 (2024) 216050.

Ran An received his Bachelor's degree in the Beijing Institute of Graphic Communication. He is now continuing his studies towards a Master's degree in the Department of Materials Science and Engineering at Beijing Jiaotong University. His current research focuses on the inverse opal photonic microspheres.

Penghui Li received his Master's degree in the China Research Institute of Daily Chemistry Co., Ltd. He is pursuing his Ph.D. in the Department of Materials Science and Engineering at Beijing Jiaotong University. His current research focuses on the multiple stopbands photonic microparticles.

Haizheng Li received his Master's degree in the Department of Materials Science and Engineering at Beijing Jiaotong University, and is now working at CRRC Changchun Railway Vehicles Co., Ltd.

Chunai Dai is a associate professor in the Department of Materials Science and Engineering at Beijing Jiaotong University. Her current research focuses on hydrogel, frost resistant coating, and liquid crystal elastomer.

Yuandu Hu is a principal investigator in the Department of Materials Science and Engineering at Beijing Jiaotong University. Prior to his current position, he accumulated more than a dozen years of research experience both in world-class academia institutions and industry organization, including the University of Notre Dame, Harvard University and EMD Electronics in the USA. He has broad research interests but his current research interests lie in the design and construction of polymer-based multifunctional materials for noise damping, sensing, anticounterfeiting, and drug delivery vehicles.